Check for updates

Multi-Factorial Comparison for 24 Distinct Transposition Models for Inclined Surface Solar Irradiance Computation in the State of Palestine: A Case Study

Yasser F. Nassar[1], Ahmed A. Hafez[2] and Samer Y. Alsadi[3*]

[1] Department of Mechanical and Industrial Engineering, Faculty of Engineering and Technology, Sebha University, Sabha, Libya, [2] Electrical Engineering Department, Faculty of Engineering, Assiut University, Asyut, Egypt, [3] Department of Electrical Engineering, Faculty of Engineering and Technology, Palestine Technical University, Tulkarem, Palestine

Solar energy industries require an accurate estimation of global solar irradiation particularly on inclined planes. This improves the accuracy of the sizing procedures and optimizes the performance of the solar energy platforms as photovoltaic modules and flat-plate solar collectors. A variety of the transposition models have been developed and reportedly determine incidences of solar irradiance on an inclined surface. However, there is a gap in the literature regarding identifying the most promising transposition model, particularly for the Middle East and North Africa region (MENA). Therefore, this article serves two main objectives. Firstly, it compares comprehensively 24 different transposition models. Several statistical methods are used to quantify the performance of the tilted surface transposition models. Furthermore, the transposition models are compared with real, hourly measured time-series data for several Palestinian cities to identify the promising and most accurate model. The analysis was carried out on three bases: annually, monthly, and a clearness index. The transposition models prove their ability to represent the measured data during the annual and monthly analyses, but they all failed to achieve complacency in the clearness index ($K_t K_t$) for the clear sky condition ($K_t > 0.78$). Secondly, the article advises a reliable and accurate transposition model for the area of the MENA for clear sky conditions. The proposed model was tested for the sites under investigation, and it produces significantly better performance than the candidate transposition models.

Keywords: diffuse, Palestine, MENA, diffuse solar irradiance, transposition models, isotropic models, anisotropic models, clearness index

INTRODUCTION

Accurate meteorological data, particularly different components of solar radiation, are mandatory for the different stages of the solar energy project, such as design, sizing, performance evaluation, and implementation phases. However, there is a lack of accurate data for the global solar irradiance on titled surfaces for the MENA region, particularly Palestine state. The transposition models could compensate for the deficiency in the measured solar irradiance data. They estimate the global solar

radiation with acceptable accuracy (Ulgen and Hepbasli, 2004; Noorian et al., 2008; Chwieduk, 2009; Besharat et al., 2013; Escobedo et al., 2014; Pandey and Katiyar, 2014; Horváth and Csoknyai, 2015; Tuomiranta and Ghedira, 2015; Michael et al., 2016; Vasar et al., 2016; Moretón et al., 2017; Zhang et al., 2017; Pérez-Burgos et al., 2018). The transposition models in general depend on the measured values of horizontal irradiance (Idh) and the global horizontal irradiance (Ih) to compute the global solar irradiance on a tilted surface. Moreover, they could be used to optimize the tilt and azimuth of Photovoltaic (PV) arrays (Yadav and Chandel, 2013; Camelia and Dorin, 2014; Khatib et al., 2015; Hafez et al., 2017; Raptis et al., 2017), which boost the conversion efficiency of PVs and allows accurate tracking for maximum power point under different operating conditions.

Recently, many transposition models are developed and reported for estimating the hourly global solar radiation on inclined surfaces. These models, as the literature claimed, could predict solar irradiation with sufficient accuracy (Ulgen and Hepbasli, 2004; Noorian et al., 2008; Tuomiranta and Ghedira, 2015; Michael et al., 2016; Moretón et al., 2017; Zhang et al., 2017). However, it is difficult to identify a promising transposition model that could be considered as a reference. The literature shows a major difference between the transposition model output and the measured data. In general, the transposition model, as the literature claimed, is site dependent. This also is obvious in **Table A1**, where list of recommended models for various countries is shown. Moreover, a discrepancy is quite obvious in the literature. For example, the isotropic model is claimed in Reindl et al. (1990a) to be the least efficient for the hourly diffusion of radiation on tilted surfaces. However, **Table A1** in the appendix shows the contrary; here, the isotropic model is adopted as a transposition model for diffuse solar irradiance on inclined plane for different countries.

Solar energy software shows the significance of transposition model accuracy. These simulation programs are developed by commercial and governmental bodies for facilitating the sizing, design, and economical/dynamic evaluation of solar energy projects. Their performance is solely transposition model dependent. Thus, uncertainty and/or inaccurate estimations of solar irradiance result in economic and technical inconveniences. **Table A2** tabulates the widely used solar energy software, including the software name, the country, and the transposition model used for developing.

Recently, several databases, such as NASA-SSE[1] SOLARGIS[2], Meteoblue AG[3], HELIOS[4], European Solar Radiation Atlas (ESRA)[5], Satel-Light[6], and Meteonorm[7], have begun to provide different components of solar irradiances, such as Ih, Idh,

and It, freely to users in a simplified manner. However, these databases face the same limitation as solar energy evaluating software; they principally depend on a transposition model. They use different models to compute the sky-diffuse and ground-reflected components of the solar irradiance on inclined surfaces. For example, the HelioClim3 database uses a Muneer model for the sky-diffuse and isotropic model for ground-reflected components[8]. Therefore, it is necessary to identify the most reliable, applicable, and accurate transposition model, which has the objective of determining the most reliable database and solar energy software.

The literature lacks clear comparative studies between the different transportation models. Usually, the literature has a peer-to-peer comparison between a proposed and an existing model. This comparison usually focuses on the ability of the proposed model to fit the measured data for a particular site and specific time span (Yadav and Chandel, 2013; Camelia and Dorin, 2014; Khatib et al., 2015; Hafez et al., 2017; Raptis et al., 2017). Therefore, this article introduces a comprehensive and statistically authenticated comparison between 24 different transposition models to identify the most promising candidate for the MENA region and the Palestine state in particular. The article addresses different problems of the widely used transposition models, such as site dependency and the mechanism for forecasting global solar irradiance on inclined surface. The analysis was carried out on three bases: annually, monthly, and a clearness index. The transposition models are compared with real, hourly measured time-series data over the course of 15 months (June 2017 to August 2018) of the selected cities to identify the promising and most accurate model. The article also advises a simple and robust transportation model for estimating the solar irradiance of inclined surface for clear sky. The MENA region enjoys a clear sky scenario, $K_t > 0.78$, for a high percentage of daylight hours.

The article has several contributions:

1. Identifying the most accurate models for representing the sky-diffuse solar irradiance under different sky conditions, and Palestinian territories are used as a case study. Consequently, the appropriate solar energy software/database could be easily determined for the study case and the similar geographical sites.
2. Advising a model that achieves better performance in predicating climatic data for clear sky than the reported transposition models. A clear sky scenario, $K_t > 0.78$, represents a high percentage of daylight hours for the region of the MENA.

DATA AND METHODOLOGY

The research methodology commenced by discussing the studied sites and the data control. This was to confirm the validity and applicability of the obtained results. Then, the transposition models concerned were highlighted. Finally, the methodology

---

[1]Satellite Solar Radiation Data. Available online at: http://www.eosweb.larc.nasa.gov/sse/.

[2]SOLAR GIS. Available online at: http://www.solargis.info/index.html.

[3]Meteoblue AG - Switzerland. Available online: http://www.meteoblue.com

[4]HELIOS. Available online: http://www.helios.ies-def.upm.es/.

[5]ESRA. The European Solar Radiation Atlas. Available online: https://www.scribd.com/document/142793445/The-European-Solar-Radiation-Atlas-Esra-1.

[6]Global radiation data based on satellite images. Available online: http://www.satellight.com.

[7]http://www.meteonorm.com/

[8]http://www.soda-pro.com/web-services/radiation/helioclim-3-archives-for-free/info

FIGURE 1 | The cities concerned in the Palestine State (circled green ●). [source: https://www.dreamstime.com/stock-illustration-state-palestine-political-map-designated-capital-east-jerusalem-claiming-west-bank-gaza-strip-borders-image74413499].

TABLE 1 | Geographical data for selected cities.

City	Latitude	Longitude	Elevation; m	Inclination of the pyranometer	Optimum tilt angle*
Rafah	31.275	34.251	75	30	23
Gaza	31.511	34.46	31	30	29
Hebron	31.528	35.094	957	30	25
Jericho	31.857	35.464	−257	30	18
Nablus	32.21	35.256	748	30	23
Tulkarm	32.302	35.021	67	30	23

Recommended by the local solar energy centers.

section introduces the statistical tools used for evaluating each transposition model individually.

Data and Studied Sites

Six different cities in the Palestine state were used for assessing the feasibility of these models. The location and geographical data for these cities are illustrated in **Figure 1** and **Table 1**. These cities are selected to represent different characteristics of the Palestine State. For example, Rafah and Gaza depict the terrains with relatively long coasts, Hebron and Nablus represent territories surrounded with mountains, and Jericho and Tulkarm represent the terrains with valleys and plains, respectively. The analysis carried out in thiss research is generic. It could therefore act as a valuable reference for similar territories.

The three components, I_{bt}, I_{dt}, and I_{rt}, of the global inclined solar irradiance It were determined from the measured values of I_t, I_h, and I_{dh}. Three pyranometers were used for values of I_t, I_h, and I_{dh}. Idh is usually obtained from an eye shaded pyranometer. This research used the data recorded from 7th June 2017 up to 12th September 2018 for Rafah, Gaza, Hebron, Jericho, Nabuls, and Tulkarm. The data of global, sky-diffuse horizontal, and global for tilt angle 30° south-facing pyranometers were recorded. A specimen of these measurements and calculations are presented graphically in **Figure 2** for horizontal and 30° south-facing planes for the four cities during the day of 21st November 2017.

Figure 2 shows that the city of Rafah receives more solar irradiance than other cities. Jericho has the highest peak. Each city has distinctive solar irradiance patterns despite the small geographical zone of them (**Figure 1**). The global inclined irradiance is more than the horizontal one, which is attributed to the reflected component. **Figure 2** shows that Gaza and Hebron have high degree of similarity. The data in the article have passed a quality control by many solar energy research centers in Gaza Strip and West Bank Universities (such as An-Najah National University, Polytechnic University, University of Palestine, The Palestinian Energy & Environment Research Center, and many others). The data are also authorized to be used by the Palestinian Central Bureau of Statistics, and they are handled by local researchers.

Transposition Models Under Concern

Transposition models require data of I_h and I_{dh} to estimate the global solar irradiance on a tilted surface (I_t). I_h is usually measured via a pyranometer. A pyranometer could be used also for measuring I_{dh} by shading its eye. This is to eliminate the direct beam component by mounting a small shading disk on the pyranometer. I_h has two components, direct beam (I_{bh}) and sky-diffuse (I_{dh}), as given by Nassar (2006), Duffie and Beckman (2013), Bilbao et al. (2014), Alsadi and Nassar (2016),

$$I_h = I_{bh} + I_{dh} \qquad (1)$$

The direct normal solar irradiance (I_{DN}) is given by

$$I_{DN} = \frac{I_{bh}}{cos\,\theta_z} \qquad (2)$$

Transposition models usually convert solar irradiance on a horizontal plane to that on a tilted one. Thus, the global irradiance for a tilted surface, I_t, at a slope angle (β) from the horizontal is given by Nassar (2006)

$$I_t = I_{bt} + I_{dt} + I_{rt} \qquad (3)$$

Equation (3) could be arranged in terms of the available data I_{bh} and I_{dh} by Nassar (2006), Duffie and Beckman (2013)

$$I_t = I_{bh}\,R_b + I_{dh}R_d + I_hR_r \qquad (4)$$
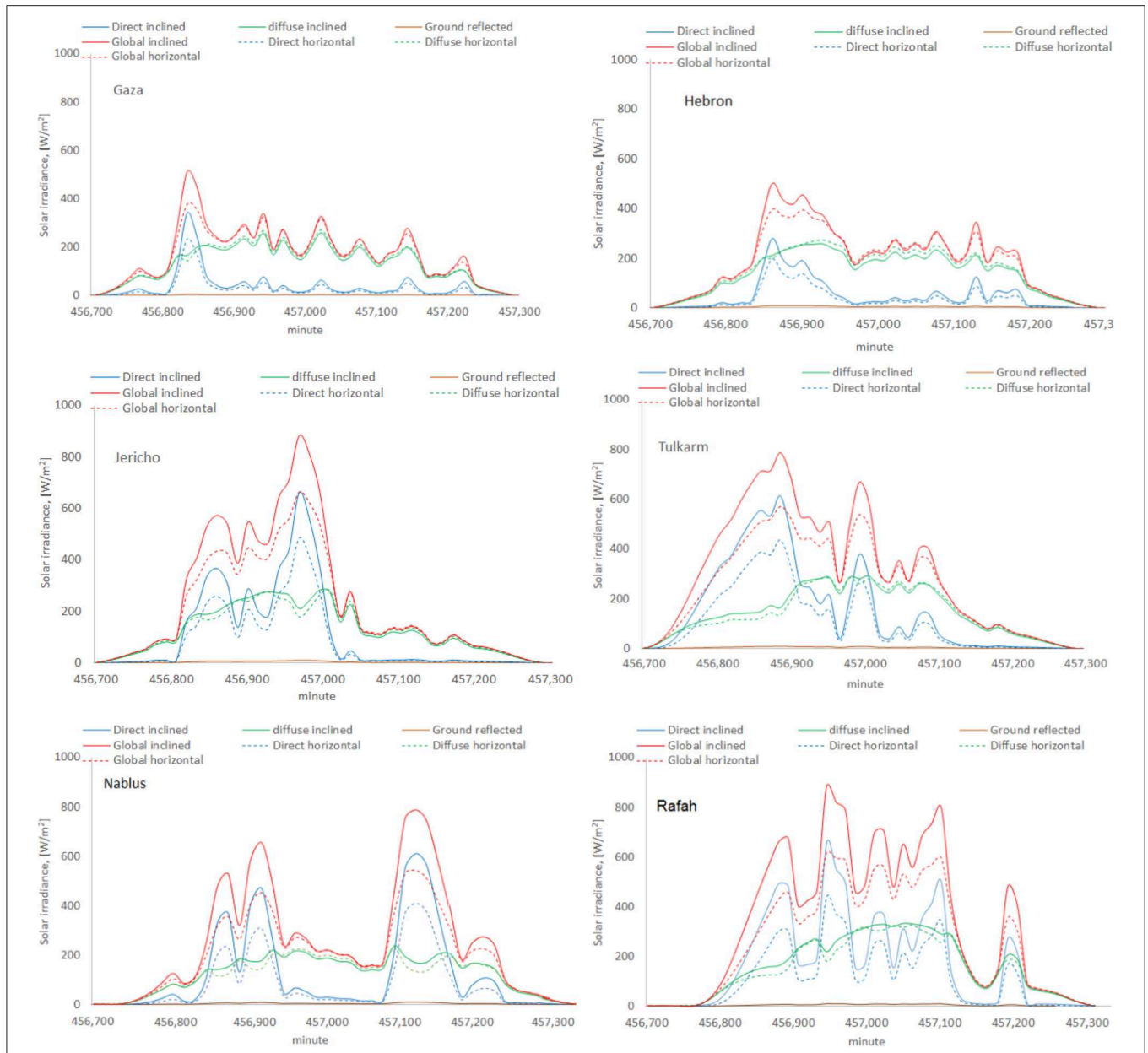
FIGURE 2 | Fifteen-minute time-series measurements and estimated solar radiation components for Gaza, Hebron, Jericho, Tulkarm, Nablus, and Rafah on November 21st, 2017.

The transposition factor R_b could be given as a function of geometrical parameters of the inclined surface and the position of the sun by Nassar (2006), Duffie and Beckman (2013)

$$R_b = max\left(0, \frac{cos\,\theta_i}{cos\,\theta_z}\right) \qquad (5)$$

where θ_i, θ_z are the solar incidence and zenith angles, respectively. Similarly, R_r is the transposition factor for ground-reflected solar irradiance. It is given by

$$R_r = p_g \frac{1 - cos\beta}{2} \qquad (6)$$

ρ_g is the albedo radiation factor, which is alternatively themed for the ground reflectivity. It is generally assumed to equal 0.2 (Moretón et al., 2017). For a ground covered with a layer of water or with plants having glossy leaves, the reflection of such radiation is usually anisotropic. The ground transposition factor R_r is given by Temps and Coulson (1977)

$$R_r = p_g \,|cos\psi|\, \left(\frac{1 - cos\beta}{2}\right)\left[1 + sin^2\left(\frac{\theta_z}{2}\right)\right] \qquad (7)$$

where ψ is the surface azimuth angle. The diffuse irradiance is due to scattering of the solar radiation by the different

components of the atmosphere. Therefore, it has naturally a non-uniform distribution throughout the sky. However, some models consider diffuse irradiance to be uniform and isotropic. Other models try to depict the scattering processing by adding to the isotropic background, the diffuse irradiance coming from the circumsolar region and the horizon band. Therefore, the models for estimating I_{dt}, and hence the transposition models, could be divided into two groups: isotropic and anisotropic. The anisotropic group is further divided depending on the region and/or the band used in considering I_{dt} (Gracia and Huld, 2013).

Isotropic Models

The isotropic models assume that the intensity of diffuse sky radiation is uniform over the sky hemisphere. Hence, the diffuse radiation depends only on the transposition factor R_d. Equations (5)–(7) could be used for determining R_b and R_r for these groups (Liu and Jordan, 1963; Temps and Coulson, 1977; Jimenez and Castro, 1986; Koronakis, 1986; Tian et al., 2001; Badescu, 2002; Nassar, 2006; Psiloglou and Kambezidis, 2009; Duffie and Beckman, 2013; Gracia and Huld, 2013; Bilbao et al., 2014; Lave et al., 2015; Alsadi and Nassar, 2016). This group includes several models:

1. *Liu and Jordan model, 1963 (Liu and Jordan, 1963),*

$$R_d = \left(\frac{1+\cos\beta}{2} \right) \tag{8}$$

2. *Korokanis model, 1986 (Koronakis, 1986),*

$$R_d = \left(\frac{2+\cos\beta}{3} \right) \tag{9}$$

3. *Jimenez & Castro model, 1986 (Jimenez and Castro, 1986),*

$$R_d = \left(\frac{1+\cos\beta}{5} \right) \tag{10}$$

The transposition factor R_b of Jimenezvand Castro model is given by (Jimenez and Castro, 1986)

$$R_b = 0.8 \frac{\cos\theta_i}{\cos\theta_z} \tag{11}$$

4. *Tian model, 2001 (Tian et al., 2001),*

$$R_d = 1 - \left(\frac{\beta}{180} \right) \tag{12}$$

where β is given in degree

5. *Badescu model, 2002 (Badescu, 2002),*

$$R_d = \frac{(3+\cos 2\beta)}{4} \tag{13}$$

Anisotropic Models

The anisotropic models assume the anisotropy of the diffuse sky radiation in the circumsolar region and the horizon in addition to the isotropic diffuse component. This group is relatively more accurate than isotropic models. Therefore, around 19 models of this group are considered in this comparative study. These include:

6. *Bugler model, 1977 (Bugler, 1977),*

$$R_d = \frac{1+\cos\beta}{2} + 0.05 \frac{I_{bh}}{I_d} R_b \tag{14}$$

7. *Temps-Coulson model, 1977 (Temps and Coulson, 1977),*

$$R_d = \left(\cos^2 \frac{\beta}{2} \right) \left(1 + \cos^2\theta_i \sin^3\theta_z \right) \left(1 + \sin^3 \frac{\beta}{2} \right) \tag{15}$$

8. *Steven and Unsworth model, 1979 (Steven and Unsworth, 1980),*

$$R_d = 0.143 \left(\sin\beta - \beta\cos\beta - \pi\sin^2\frac{\beta}{2} \right) + \cos^2\frac{\beta}{2} \tag{16}$$

9. *Hay model, 1979 (Hay, 1979),*

$$R_d = F_{Hay} R_b \left(1 - F_{Hay} \right) \left(\frac{1+\cos\beta}{2} \right) \tag{17}$$

where $F_{Hay} = \left(\frac{I_{bh}}{I_{ext}} \right)$ is Hay's sky-clarity factor

10. *Klucher model, 1979 (Klucher, 1979),*

$$R_d = \left(\cos^2\frac{\beta}{2} \right) \left(1 + f_k\cos^2\theta_i \sin^3\theta_z \right) \left(1 + f_k\sin^3\left(\frac{\beta}{2}\right) \right) \tag{18}$$

where $f_k = 1 - \left(\frac{I_{dh}}{I_h} \right)^2$

11. *Modified Steven and Unsworth model, 1980 (Steven and Unsworth, 1979),*

$$R_d = 0.51 R_b + \frac{1+\cos\beta}{2} - \frac{1.74}{1.26\pi} \left[\sin\beta - \beta\cos\beta - \pi\sin^2\frac{\beta}{2} \right] \tag{19}$$

12. *Willmot model, 1982 (Willmot, 1982),*

$$R_d = \frac{I_{bn} R_b}{I_0} + C_\beta \left(1 + \frac{I_{bn}}{I_{sc}} \right) \tag{20}$$

where: $Ibn = \frac{I_b}{\cos\theta_z}$, $C_\beta = 1.0115\ 0.20293\beta\ 0.080823\beta^2$, β is in radians, and $I_{sc} = 1367 \text{W/m}^2$

13. *Ma-Iqbal model, 1983 (Ma, 1983),*

$$R_d = k_t R_b \left(1 - k_t \right) \left(\frac{1+\cos\beta}{2} \right) \tag{21}$$

where k_t is the clearness index $k_t = \frac{I_h}{I_{ext}}$

14. *Skartveit-Olseth model, 1986 (Skartveit and Olseth, 1986),*

$$R_d = F_{Hay} R_b + Z\cos\beta + \left(1 - F_{Hay} - Z \right) \cos^2\left(\frac{\beta}{2} \right) \tag{22}$$

where $Z = max \left[\left(0.3 - 2F_{Hay} \right), 0 \right]$.

Equations (17) and (22) show that the Skartveit-Olseth model is evolved from the Hay model. Therefore, the performances of these models are forecasted to have a high degree of similarity.

15. *Gueymard model, 1987 (Gueymard, 1986),*

$$R_d = (1-N_g) R_{d0} + N_g R_{d1} \qquad (23)$$

where N_g, R_{do} and R_{d1} are given by

$$N_g = \max\left[\min(Y,1),0\right] \qquad (24)$$

$$Y = \begin{cases} 6.6667 \frac{I_{dh}}{I_h} - 1.4167 & if \ \left(\frac{I_{dh}}{I_h}\right) \le 0.227 \\ 1.2121 \frac{I_{dh}}{I_h} - 0.1758 & other\ wise \end{cases} \qquad (25)$$

$$R_{d0} = \exp\left(a_0 + a_1 \cos\theta + a_2 \cos^2\theta + a_3 \cos^3\theta\right) \\ + F(\beta)\, G(\gamma) \qquad (26)$$

where coefficients a_i are a function of the solar elevation angle in γ degrees,

$$a_0 = 0.897\ \ 3.364\gamma' + 3.96\ \gamma'^2\ \ 1.909\gamma'^3 \qquad (27)$$

$$a_1 = 4.448\ \ 12.962\ \gamma' + 34.601\ \gamma'^2\ \ 48.784\gamma'^3 \\ + 27.511\ \gamma'^4 \qquad (28)$$

$$a_2 = 2.77 + 9.164\ \gamma'\ 18.876\ \gamma'^2 \\ + 23.7764\gamma'^3\ 13.041\gamma'^4 \qquad (29)$$

$$a_3 = 0.312\ \ 0.217\gamma'\ 0.805\ \gamma'^2 + 0.318\ \gamma'^3 \qquad (30)$$

where $\gamma' = 0.01\gamma$

$$F(\beta) = \frac{1\ \ 0.2249 \sin^2\beta + 0.1231 \sin 2\beta + 0.0342 \sin 4\beta}{1\ \ 0.2249} \qquad (31)$$

$$G(\gamma) = 0.408\ \ 0.323\ \gamma' + 0.384\ \gamma'^2 - 0.17\ \gamma'^3 \qquad (32)$$

$$R_{d1} = \frac{1+\cos\beta}{2} - \frac{\frac{1}{\pi}\ (\beta\cos\beta - \sin\beta) + \left(\frac{1-\cos\beta}{2}\right)}{\left(1+ \frac{3}{2b}\right)} \qquad (33)$$

where b = 1.5

16. *Modified Bugler model, 1988 (Hay and McKay, 1988),*

$$R_d = \left(1 - 0.05\frac{I_{bh}}{I_d}\right)\frac{1+\cos\beta}{2} + 0.05\frac{I_{bh}}{I_d}R_b \qquad (34)$$

17. *Perez model, 1988 (Perez and Scott, 1983; Perez and Stewart, 1983; Perez and Arbogast, 1985; Perez et al., 1986, 1987a,b, 1990a,b),*

The Perez model is subjected to continuous revisions. This is to improve its performance capabilities and fit the measured data more accurately (Perez and Scott, 1983; Perez and Stewart, 1983; Perez and Arbogast, 1985; Perez et al., 1986, 1987a,b, 1990a,b). In this research study, two versions of the perez models are investigated: Perez model 1988 and1990. Perez model 1988, is given by

$$R_d = F_1 \frac{a}{b} + (1-F_1)\left(\frac{1+\cos\beta}{2}\right) + F_1\ \sin\beta \qquad (35)$$

where a, b, F_1, and F_2 are given by

$$a = \max(0, \cos\theta_i) \qquad (36)$$
$$b = max\left(\cos 85^o, \sin\gamma\right) \qquad (37)$$
$$F_1 = F_{11}(\varepsilon) + F_{12}(\varepsilon\Delta) + F_{13}(\varepsilon)\ \theta_z \qquad (38)$$
$$F_2 = F_{21}(\varepsilon) + F_{22}(\varepsilon\Delta) + F_{23}(\varepsilon\Delta)\ \theta_z \qquad (39)$$

where $\varepsilon = \frac{\frac{I_h}{I_{dh}} + 1.041\theta_z^3}{1 + 1.041\theta_z^3}$ and $\Delta = M\frac{I_{dh}}{I_{ext}}$, θ_z is in radians, and M is the optical air mass.

Perez published many versions of the F_{ij} coefficients for different locations. **Table A3** tabulates the F_{ij} coefficients for Perezs model 1988.

18. *Perez model, 1990 (Perez and Scott, 1983; Perez and Stewart, 1983; Perez and Arbogast, 1985; Perez et al., 1986, 1987a,b, 1990a,b),*

Perez model 1990 reported in the literature (Perez et al., 1987a,b) has the same equations as Perez model 1988, Equation (35)–(39). However, the values of F_{ij} coefficients, and thus F_{ij} coefficients, differ from those in **Table A3**. **Table A4** gives the F_{ij} coefficients for Perezs model 1993.

19. *Modified Ma-Iqbal model, 1990 (Kasten, 1966),*

$$R_d = k_t' R_b + (1 - k_t')\left(\frac{1+\cos\beta}{2}\right) \qquad (40)$$

Where k_t' and the optical air mass, M are given, respectively, by

$$k_t' = \frac{k_t}{1.031 \exp\left(\frac{-1.4}{0.9 + \frac{9.4}{M}}\right) + 0.1} \qquad (41)$$

$$M = \left[\cos\theta_z + 0.15(93.885 - \theta_z)^{-1.253}\right]^{-1} \qquad (42)$$

k_t is as given by Equation (21)

20. *Muneer model, 1990 (Muneer, 1990, 1997; Muneer et al., 2004),*

$$R_d = TM\ (1-F_M) + F_M R_b \qquad (43)$$

$$TM = \left(\frac{1+\cos\beta}{2}\right) \\ + \frac{2b}{\pi\ (3+2b)}\left(\sin\beta - \beta\cos\beta - \pi \sin^2\left(\frac{\beta}{2}\right)\right) \qquad (44)$$

F_M is a composite clearness function. For shaded surface or overcast sky conditions $F_M = 0$ and b = 2.5, while for clear sky and partly cloudy sky conditions $F_M = F_{Hay}$ and F_{Hay} could be determined by solving the following quadratic equation

$$F_{Hay}^2 + 0.404\ F_{Hay} + \left(\frac{0.987b}{\pi\ (3+2b)} - 0.0197\right) = 0.0 \qquad (45)$$

21. *HDKR model, 1990 (Reindl et al., 1990a,b):*

$$R_d = F_{Hay}R_b + \left(1 - F_{Hay}\right)\left(\frac{1+cos\beta}{2}\right)\left[1 + f sin^3\left(\frac{\beta}{2}\right)\right] \quad (46)$$

where $f = \sqrt{\left(\frac{I_{bh}}{I_h}\right)}$

22. *Hay model, 1993 (Hay, 1993):*

$$R_d = F_{Hay}'R_b + \left(1 - F_{Hay}'\right)cos^2\left(\frac{\beta}{2}\right) \quad (47)$$

Where $F_{Hay}' = \frac{I_{bh}}{I_{sc}}$

This late model of Hay 1993 is the modified version of Hay's 1979. However, Hay's factor F_{Hay} in Equation (47) is normalized to the maximum value of solar irradiance, I_{sc}.

23. *Modified Olmo model, 1999 (Olmo et al., 1999),*

$$R_d = \exp\left(-k_t\left(\theta_i^2 - \theta_z^2\right)\right)f_c' \quad (48)$$

where θ_i and θ_z (in radians) are the incidence and solar zenith angles, respectively, k_t is the hourly clearness index, and the ρ_g is albedo of the underlying surface. The function f_c' is given by

$$f_c' = \begin{cases} 1 - \rho_g \, cos^3\frac{\theta_i}{2} & if \ 0 \le k_t \le 0.35 \\ 1 - \rho_g \, sin\frac{\theta_i}{2} & if \ 0.35 \le k_t \le 0.65 \\ 1 & otherwise \end{cases} \quad (49)$$

24. *CIBSE model, 2008 (CIBSE, 2008),*

This is a modification of Klucher model, where the diffuse horizontal radiation was corrected:

$$I_{dh}' = I_{dh} \, x \, f_\beta \left(1 - k_b\right) + k_b \, R_b \quad (50)$$

where k_b and f_β are given by

$$k_b = \frac{I_{bh}}{\epsilon_j I_{ext}} \quad (51)$$

$$f_\beta = \left[cos^2\frac{\beta}{2} + \left\{\frac{2c}{\pi(3+2c)}\right\} x \left\{sin\beta - \frac{\pi\beta}{180}\right\}cos\beta\right.$$
$$\left. - \pi sin^2\frac{\beta}{2}\right] \quad (52)$$

ϵ_j is the correction to mean solar distance on day j, and c is a constant. The values for constant c are as follows: Shadow surface: c = 5.73, Sunlit surface under overcast sky: c = 1.68, and Sunlit surface under non-overcast sky: c = −0.62.

Transposition Models Assessment

Four different statistical methods are used to assess the potential of the transposition models. This is to identify the most reliable and accurate model, particularly for the area under concern. RMSE, MBE, PAD, and t-stat are the tools of the comparison. Furthermore, the outputs of the different transposition models are compared with measured values to visualize the fitting ability

of each model. RMSE, MBE, PAD, and t-stat are defined by Alsadi and Nassar (2016),

$$RMSE = \left[\frac{1}{n}\sum_{i=1}^{n}\left(I_{i,c} - I_{i,m}\right)^2\right]^{1/2} \quad (53)$$

$$MBE = \frac{1}{n}\sum_{i=1}^{n}\left(I_{i,c} - I_{i,m}\right) \quad (54)$$

$$PAD(\%) = \frac{100}{n}\sum_{i=1}^{n}\frac{\left|I_{i,c} - I_{i,m}\right|}{I_{i,c}} \quad (55)$$

$$t - stat = \left[\frac{(n-1)\,MBE^2}{RMSE^2 - MBE^2}\right]^{1/2} \quad (56)$$

The statistical methods Equations (53)–(56) could provide a logical pattern for comparing the different models. The Equations (53)–(56) indicates that the smaller values of RMSE, PAD, and t-stat the more accurate the transposition models are. The Equations (53)–(56) show that the results of RMSE, PAD, and t-stat are positive, while MBE produce ± values according to the deviation of the estimate from the measured values. The most promising transposition model should have the smallest values for RMSE, MBE, PAD, and t-stat simultaneously. However, they may not agree simultaneously on single transposition model (Khan and Ahmad, 2012). Therefore, the graphical comparison is introduced to show visually the correlation between the measured values and the output of each model.

RESULTS AND DISCUSSION

The analysis is carried according to three bases: annual, monthly, and a clearness index. This diversity in the analysis widens the comparison and thus increases the feasibility and reliability of the conducted results.

All Sky Conditions (Annual) Base Analysis

The evaluation was carried out on an hourly basis for almost 1 year's worth of data records. The sky-diffuse solar irradiance on a 30° tilted south-facing surface was determined from measured horizontal data using the 24 models and compared with the semi-measured data for a tilted surface during the same period. **Table 2** tabulates the statistical analysis results of the 24 considered transposition models for Hebron city.

Skartveit-Olseth and HDKR are the most promising candidates according to RMSE. For t-stat, Perez 1990 has the best performance; however, HDKR is a reliable candidate. According to MBE, Perez 1990 is the most accurate model for Herbon city. It is clear from **Table 2** that there is a difficulty for a model to achieve the best performance according to the different comparison statistical tools simultaneously. It could be concluded that HDKR model produces the better overall performance than the others for Herbon city. The table mandates the application of an additional comparison tool in order to confirm the feasibility and applicability of a definite transposition model. This tool could be the graphical comparison between the

TABLE 2 | Results of the transposition models, for Hebron city for a tilted angle of 30° south facing.

No	Transposition model	RMSE, (W/m²)	MBE, (W/m²)	PAD%	t-stat
1	Liu and Jordan	13.58	−6.22	6.94	2.47
2	Korokanis	12.36	−4.96	6.24	2.10
3	Badescu	17.41	−9.49	9.75	3.12
4	Tian	20.54	−11.83	12.37	3.38
5	Jimenez & Castro	59.84	−37.74	88.47	3.90
6	Willmot	47.88	31.87	3.66	4.28
7	Gueymard	12.27	2.06	3.52	15.98
8	Bugler	14.52	1.98	4.68	0.66
9	M. Bugler	12.67	−6.28	4.30	2.73
10	Ma-Iqbal	11.18	6.70	3.23	3.59
11	M. Ma-Iqbal	15.04	10.41	6.72	4.60
12	Steven and Unsworth	22.49	−13.57	11.89	3.63
13	M. Steven&Unsworth	52.46	28.70	14.92	3.13
14	Hay (1979)	8.89	−3.30	1.42	1.92
15	Hay (1993)	10.84	−5.06	3.30	2.53
16	HDKR	8.79	−2.96	1.25	1.72
17	Skartveit-Olseth	8.96	−3.43	1.50	1.99
18	Muneer	37.15	−20.50	35.68	3.17
19	Temps-Coulson	59.04	−37.79	76.54	4.00
20	M. Olmo	14.32	0.53	4.03	0.18
21	Klucher	10.91	0.66	2.81	0.29
22	CIBSE	12.750	3.54	4.44	27.03
23	Perez et al. (1988)	16.86	−5.81	7.77	1.76
24	Perez et al. (1990a)	12.71	−0.19	5.24	0.07

model output and the measured data (Padovan and Del-Col, 2010; Besharat et al., 2013).

In the graphical comparison, **Figure 3**, the red line represents the locus of the ideal transposition model. Therefore, the quality of a transposition model performance is evaluated via the shape of the distribution of blue dots around the red line. The average of the blue dots should be as close as possible to the red line for a reliable transposition model. **Figure 3** shows that the majority of transposition model could produce reasonable accuracy in predicting I_{dt} for Herbon city. However, HDKR, Skartveit-Olseth, and Hay 1979 are the most promising models. Meanwhile, Jimenez and Castro, Muneer, Temps-Coulson, and M. Steven deviated significantly from the measured values.

It could be concluded from **Table 2** and **Figure 3** that HDKR could be considered as the reference transposition model for Herbon city.

Table 2 shows that t-stat is the least efficient comparison tool as it diverges from the remaining tools. Moreover, the graphical comparison, **Figure 3**, validates the deficiency of t-stat. The authors, when assessing the transposition models in the other cities concerned, found again that t-stat could not identify the promising model. Therefore, it could be concluded that t-stat is not recommended for identifying a transposition model for particular zone. This, however, differs from the conclusion in reference (Togrul, 1989), which recommends adopting t-stat as the standard tool for determining the best transposition model.

Also, MBE fails to identify the appropriate transposition model for a specific city/zone. **Table 2** and **Figure 3** validate this finding. Therefore, RMSE and PAD are only considered in the remaining research as the authenticated comparative tools. The results of RMSE and PAD of different transposition models for different cities under investigations are given in **Table 3**.

Table 3 shows that there is coherent between RMSE and PAD. For a transposition model they converge simultaneously to optimal solutions. They could therefore also identify the quality of the transposition model at the same time. The bold numbers in **Table 3** show the best solution. HDKR is the most promising solution for 83% of territories under concern. Again, Hay 1979 and Skartveit-Olseth produced comparable performance to HDKR at the majority of the cities under concern. Skartveit-Olseth produced better results than HDKR at Nablus. The preferred transposition models for Gaza, Rafah, Jericho, Tulkram, and Nablus are shown in **Figure 4**, where a visual comparison between estimated and measured values of I_{dt} for these cities is shown.

Figure 4 shows that HDKR model is the most accurate for majority of cities under concern except Nablus where the Stratveit-Olseth model is the most accurate model.

Monthly Based Analysis

The monthly based approach was adopted to improve the accuracy of the obtained results. PAD was the tool used in the monthly based analysis to differentiate between the different transposition models. Again, the analysis was carried out from August 2017 until September 2018 for six different cities in the Palestine State. **Table 4** shows the most promising transposition model for the different cities during each month.

Table 4 confirms the annually based analysis, as HDKR is the most promising candidate at different sites except Nablus, where Skartveit-Olseth model is preferred. However, there was some disparity in the behavior of the models over the months. The similarity between Rafah and Gaza is attributed to same climatological conditions for the two cities.

Clearness Index (Kt) Based Analysis

This analysis assesses the ability of the different transposition models in manipulating solar irradiance for different sky conditions. The sky conditions are classified into three scenarios (Burgess et al., 2011): overcast, intermediate, and clear conditions. The clearness index, k_t, usually differentiated between the different conditions the sky. For example, overcast condition clearness index is below 0.3, $k_t < 0.3$, while for intermediate conditions the clearness index is between 0.3 and 0.78 $0.3 \leq k_t \leq 0.78$, and clearness index is more than 0.78, $k_t > 0.78$ for clear conditions. The RMSE and PAD were calculated for all cities under different values of k_t. The most accurate models having the lowest value of the RMSE and PAD are given in **Table 5**.

Table 5 again shows that there is no single transposition model that could produce an accurate estimation for the global solar irradiance on a titled plane and its component for different sky conditions, even for the same city. HDKR produced a satisfactory performance for intermediate sky condition for all cities except Nablus. However, for overcast and clear conditions, HDKR
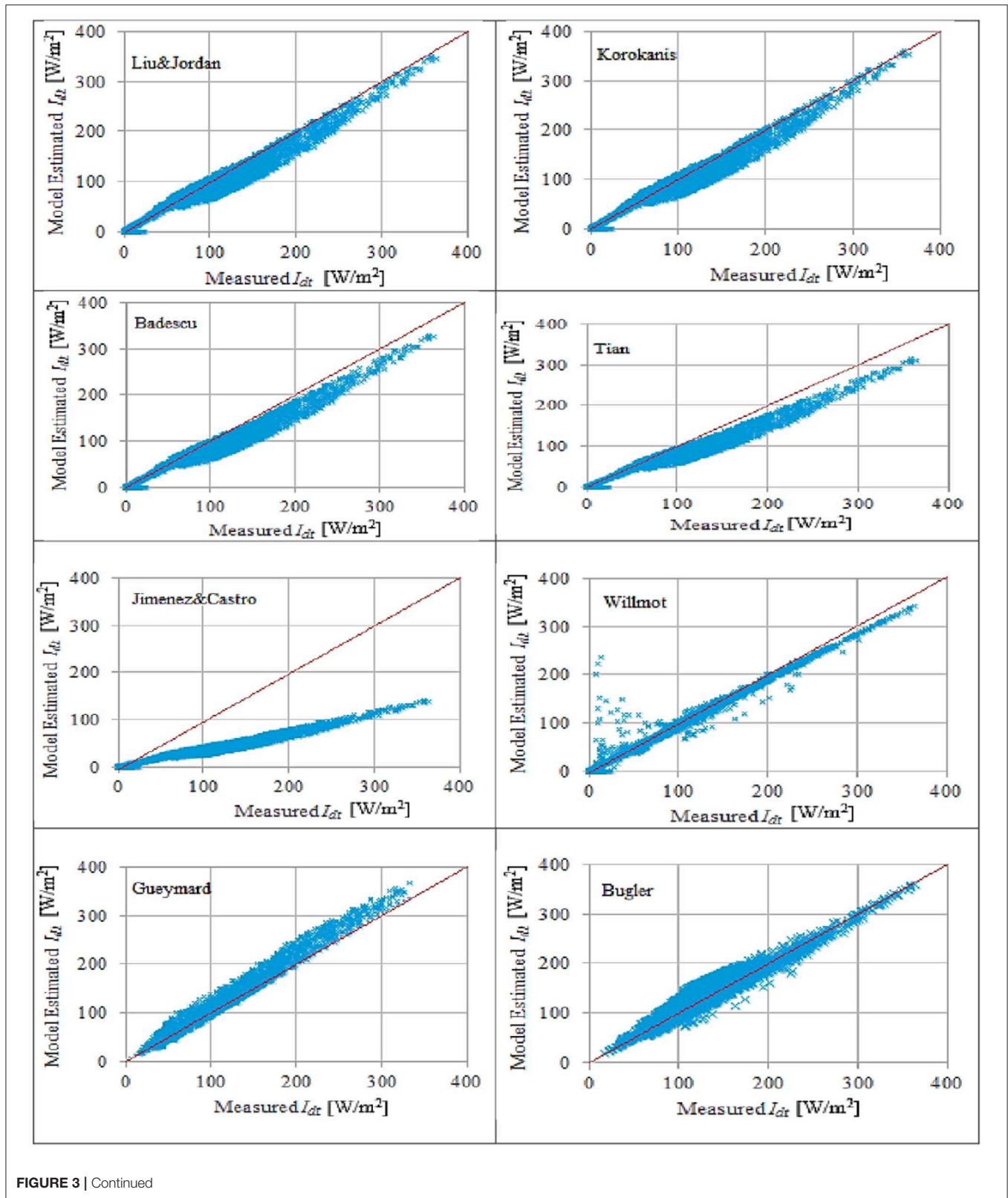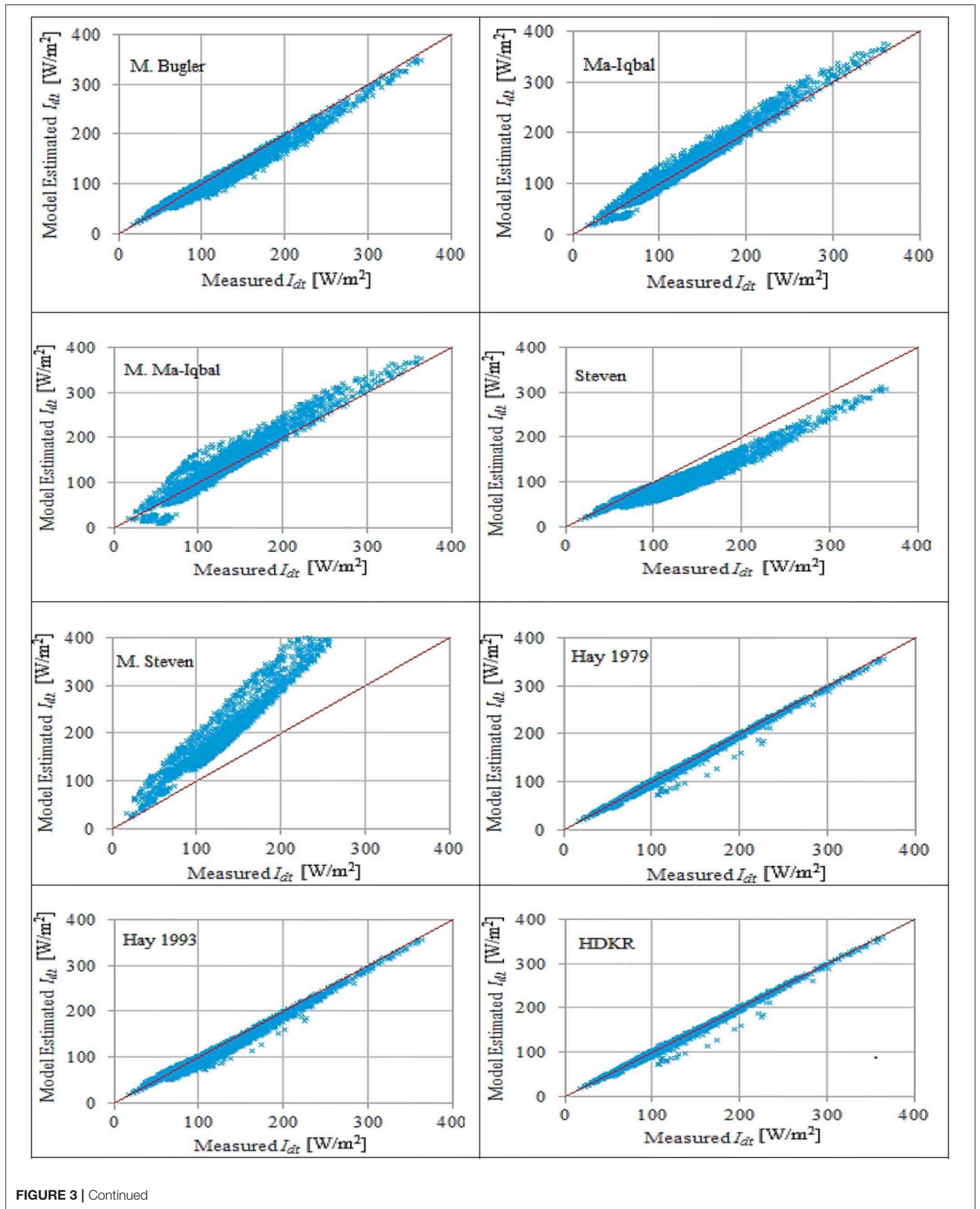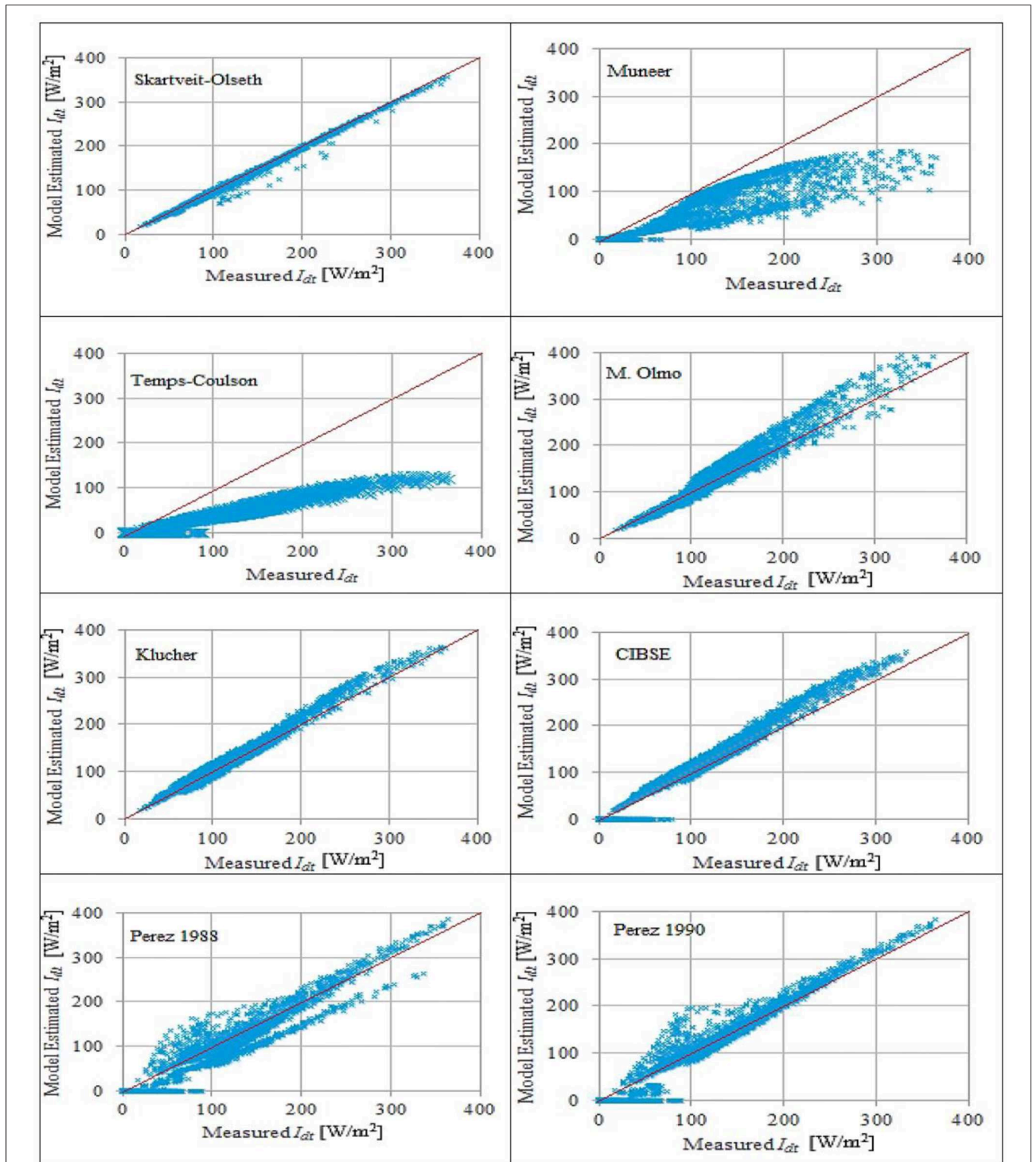
FIGURE 3 | Continued

FIGURE 3 | Continued

FIGURE 3 | Sky-diffused solar irradiance estimation vs. measures for south-facing 30° tilt angle inclined surface in Herbon city for 24 models during all sky conditions (8,700 points depicted in the graph) (blue dot), y = x relation (red line).

TABLE 3 | RMSe and PAD of transposition models considered cities for a surface tilted 30° south facing.

Transposition model	West bank								Gaza strip			
	Hebron		Jericho		Tulkarm		Nablus		Rafah		Gaza	
	RMSE	PAD%	RMSE	PAD%	RMSE	PAD%	RMSE	PAD%	RMSE	PAD%	RMSE	PAD%
Liu and Jordan	13.58	6.94	13.82	5.36	13.27	5.85	11.52	6.26	14.16	6.03	13.70	6.00
Korokanis	12.36	6.24	12.40	4.76	11.98	5.28	10.89	6.05	12.74	5.30	12.38	5.36
Badescu	17.41	9.75	18.27	8.20	17.50	8.62	14.47	7.61	18.52	9.03	17.90	8.91
Tian	20.54	12.37	21.84	10.96	20.97	11.32	17.33	9.53	22.00	11.82	21.31	11.68
Willmot	29.70	3.66	36.50	3.44	26.99	3.28	4.07	2.17	26.41	3.85	35.51	3.61
Bugler	14.52	4.68	13.58	3.74	13.14	3.69	14.35	4.97	13.84	3.80	13.31	3.58
M. Bugler	12.67	4.30	13.16	3.71	12.52	3.84	10.42	3.62	13.60	4.09	13.05	3.98
Ma-Iqbal	11.18	3.23	11.33	3.29	11.27	3.20	12.27	3.52	11.53	3.17	11.24	3.09
M. Ma-Iqbal	15.04	6.72	15.51	5.52	15.34	5.76	16.07	6.41	15.49	5.72	15.06	5.63
Steven	22.49	11.89	23.64	10.55	22.82	10.92	19.02	9.43	23.99	11.33	23.26	11.25
Hay (1979)	8.89	1.42	8.55	1.22	8.51	1.21	7.93	1.48	9.29	1.45	9.03	1.34
Hay (1993)	10.84	3.30	10.49	2.56	10.38	2.76	9.06	2.74	11.19	2.93	10.85	2.86
HDKR	8.79	1.25	8.41	1.03	8.40	1.06	8.12	1.53	9.12	1.22	8.88	1.16
Skartveit-Olseth	8.96	1.50	8.64	1.28	8.57	1.21	7.81	1.38	9.35	1.54	9.09	1.41
Modified Olmo	14.32	4.03	64.48	74.16	14.86	3.94	15.23	3.93	15.20	4.13	14.60	4.05
Klucher	10.91	2.81	15.27	4.09	11.14	2.65	12.75	3.86	11.15	2.41	11.00	2.42
Perez et al. (1988)	16.86	7.77	19.31	8.18	18.24	8.33	16.80	12.96	18.72	21.75	18.11	6.63
Perez et al. (1990a)	12.71	5.24	13.44	5.48	13.34	4.72	13.65	5.18	13.42	5.10	13.30	4.95

deviated from the optimal performance. The Perez model is possibly preferred for a clear sky, while Hay is preferable for overcast.

Table 5 shows that all cities except Nablus and Tulkram have the same best models: Hay 1979, HDKR, and Perez 1900 for clear, intermediate, and overcast sky conditions, respectively. This could be attributed to the latitudes of Nablus and Tulkram, as shown in **Figure 1** and **Table 1**. These two cities are relatively far from the remaining cities.

The preferred models, **Table 5**, are subjected to the graphical comparison with the measured data for Hebron **Figure 5** and Nablus **Figure 6**. Hebron and Nablus represent the two extremes.

Figures 5, **6** show the preferred models have satisfactory prediction capabilities for the measured data. However, for clear sky, kt > 0.78, the prediction capabilities of Perez 1990 and Ma-Iqbal were not adequate.

Perez 1990 and Ma-Iqbal models were the preferred models for Hebron and Nablus, respectively, for kt > 0.78, **Table 5**. However, their performances in the graphical comparison were not efficient. Moreover, kt > 0.78 represents the most dominant weather conditions in the area of MENA and Palestine State. Therefore, an adequate and robust transposition model is advised in this research for kt > 0.78.

ADVISED TRANSPOSITION MODEL FOR CLEAR SKY, $K_T > 0.78$

The proposed model is basically a modification of the Muneer model. It is realized by increasing the share of the isotropic term in Equations (41) and (42). Different regression methods are used

for developing the proposed model. Then, a refining is carried out to the model via trial and error technique. The proposed model is given by

$$R_d = T_{Mp} \left(1 - F_p\right) + F_p R_b \tag{57}$$

$$T_{Mp} = \left\{ 16.7362 + \frac{17.5317}{\left[1 + \exp\left(\frac{0.97 - \beta}{0.1689}\right)\right]^{0.008}} \right\} \tag{58}$$
$$+ \frac{2b}{\pi \left(3 + 2b\right)} \left(\sin\beta - \beta\cos\beta - \pi\sin^2\left(\frac{\beta}{2}\right)\right)$$

F_b is as mentioned before a composite clearness function. It is equal to F_{Hay}, which is obtained from Equation (42) and is given in radians.

Table 6 tabulates the performance of the proposed model is compared against the best models for the different cities under investigations for clear sky conditions, $k_t > 0.78$. RMSE and PAD are used as the comparison tools.

Table 6 shows that the proposed model is better at predicating sky-diffused solar irradiance on a titled surface for a clear sky than reported transposition models. There is around 600% reduction in the values of RMSE and PAD. This indicates that the proposed model outputs are similar to the measured values. **Table 6** corroborates the reliability and functionality of the proposed model. The feasibility of the proposed model is validated further via a graphical comparison with the measured data, as shown in **Figure 7**.

Figure 7 shows the applicability of the proposed model in predicting global diffused solar irradiance on a titled surface. It fits the measured data efficiently.
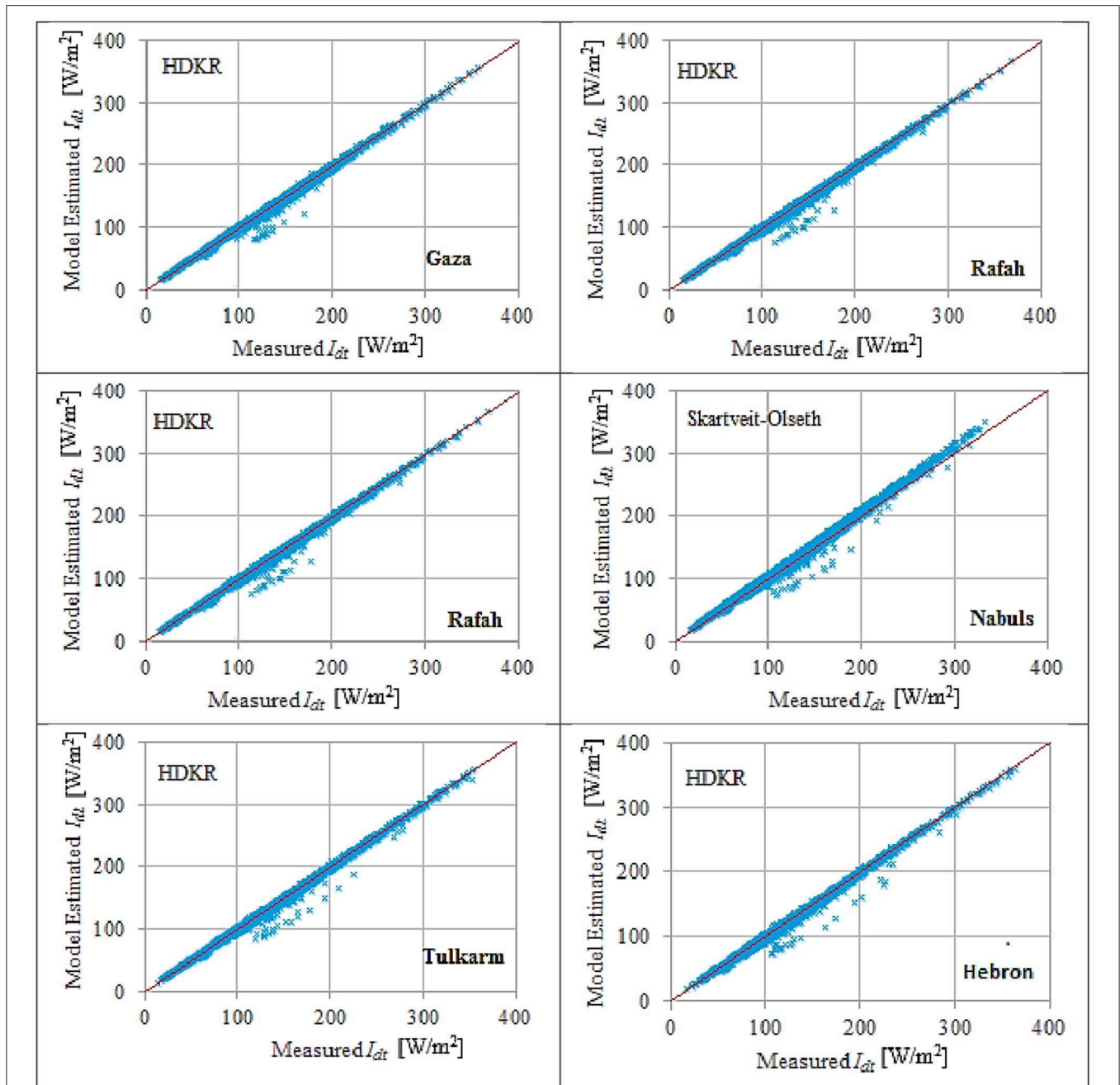
FIGURE 4 | The most accurate diffuse-sky solar irradiance transposition models for the considered cities (8,700 points depicted in the graph) (blue dot), y = x relation (red line).

Comparing **Figures 5**–**7** reveals the evaluated quality of the proposed model. It produces much higher quality than even the best models. This model could be considered as a reference for Palestine city under investigations for this 30° south-facing inclined surface. Moreover, the feasibility of the proposed model is examined in other cities for the same climatological conditions. It again produces the best performance for clear sky condition, $k_t > 0.78$.
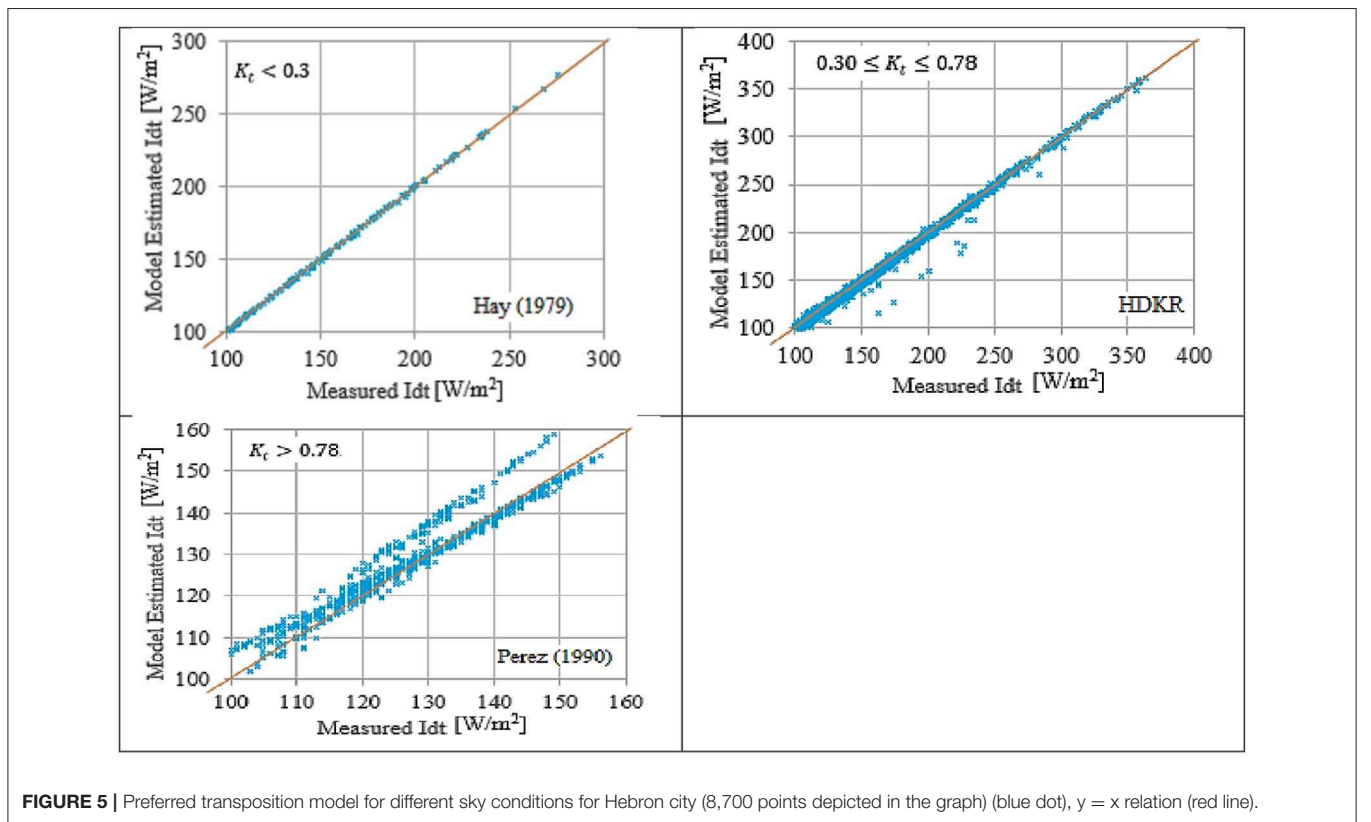
CONCLUSION

The transposition model is a basic element in the solar energy conversion systems. It generates the data of the incidence of different solar irradiance components on inclined surfaces. These data are mandatory for the phases of design, sizing, and implementation of a solar energy project.

TABLE 4 | The monthly preferred model for each city from August 2017 until September 2018.

Month	Hebron	Jericho	Tulkarm	Nablus	Rafah	Gaza
January	HDKR	Ma-Iqbal	Hay (1979)	Skartveit-Olseth	HDKR	HDKR
February	HDKR	HDKR	HDKR	Skartveit-Olseth	HDKR	HDKR
March	HDKR	HDKR	HDKR	Skartveit-Olseth	HDKR	HDKR
April	Ma-Iqbal	HDKR	HDKR	Willmot	M.Ma-Iqbal	Ma-Iqbal
May	HDKR	HDKR	HDKR	HDKR	Hay (1993)	HDKR
June	HDKR	HDKR	HDKR	HDKR	M. Bugler	M.Bugler
July	HDKR	HDKR	HDKR	HDKR	Hay (1993)	Hay (1993)
August	HDKR	HDKR	HDKR	Ma-Iqbal	HDKR	HDKR
September	Ma-Iqbal	HDKR	HDKR	Skartveit-Olseth	HDKR	HDKR
October	HDKR	HDKR	HDKR	Skartveit-Olseth	HDKR	HDKR
November	HDKR	HDKR	HDKR	Skartveit-Olseth	HDKR	HDKR
December	HDKR	Ma-Iqbal	Skartveit-Olseth	Willmot	HDKR	HDKR

TABLE 5 | The best transposition models For different Kt.

Clearness index	Hebron	Jericho	Tulkarm	Nablus	Rafah	Gaza
$K_t < 0.30$	Hay (1979)	Hay (1979)	Skartveit-Olseth	Willmot	Hay (1979)	Hay (1979)
$0.30 \leq K_t \leq 0.78$	HDKR	HDKR	HDKR	Skartveit-Olseth	HDKR	HDKR
$K_t > 0.78$	Perez (1990)	Perez (1990)	Perez (1990)	Ma-Iqbal	Perez (1990)	Perez (1990)

FIGURE 5 | Preferred transposition model for different sky conditions for Hebron city (8,700 points depicted in the graph) (blue dot), y = x relation (red line).

Solar energy software is usually developed according to specific transposition model. Moreover, the databases employ transposition models to generate the different solar irradiance data. Therefore, evaluating the performance of the dominant transposition models is elementary in determining the appropriate database and solar software.
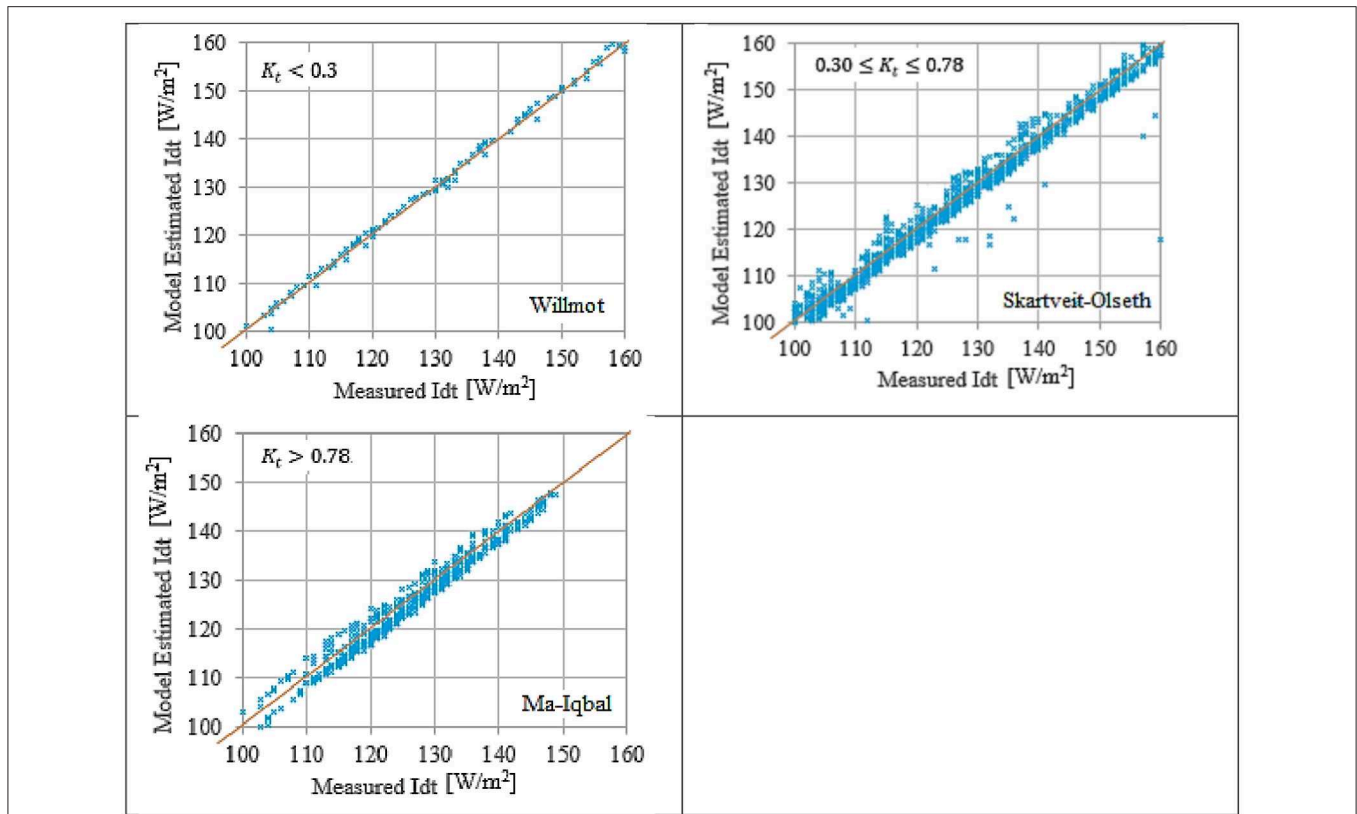
FIGURE 6 | Preferred transposition model for different sky conditions for Nablus city (8,700 points depicted in the graph) (blue dot), y = x relation (red line).

TABLE 6 | The best and Proposed model For clear sky Kt > 0.78.

Transposition model	City/best model											
	Hebron/Perez 1990		Jericho/Perez 1990		Tulkarm/Perez 1990		Nablus/Ma-laqbal		Rafah/Perez 1990		Gaza/Perez 1990	
	RMSE	PAD%	RMSE	PAD%	RMSE	PAD%	RMSE	PAD%	RMSE	PAD%	RMSE	PAD%
Best model	6.76	5.94	3.61	1.92	4.50	1.03	3.95	2.77	4.99	1.19	3.94	1.20
Proposed model	1.02	1.79	2.90	1.69	1.92	0.68	1.02	2.06	2.48	0.63	1.42	0.44

This article compared comprehensively 24 different transposition models. The comparison is multi-factorial; it includes statistical and graphical phases. In the statistical part, four different methods—RMSE, MBE, PAD, and t-stat—were used to identify the most promising transposition model. In the graphical, the outputs of the transposition models were compared with the measured data to visualize the accuracy of the different models. Moreover, the comparison was carried out on three bases: annual, monthly, and a clearing index. Climatological data over 15 months (June 2017 to August 2018) of six different cities in the Palestine State were used to identify the potential of these 24 models, thus identifying the most accurate model for this region.

The results reveal a number of conclusions:

1. The Transposition model is site dependent; it is therefore difficult to adopt one model for entire zone/region with diverse climatological conditions. This conclusion complies with the literature (Kasten, 1966; Bugler, 1977; Hay, 1979, 1993; Klucher, 1979; Steven and Unsworth, 1979, 1980; Willmot, 1982; Ma, 1983; Perez and Scott, 1983; Perez and Stewart, 1983; Perez and Arbogast, 1985; Gueymard, 1986; Perez et al., 1986, 1987a,b, 1988, 1990a,b; Skartveit and Olseth, 1986; Hay and McKay, 1988; Muneer, 1990, 1997; Reindl et al., 1990b; Olmo et al., 1999; Tian et al., 2001; Badescu, 2002; Muneer et al., 2004; CIBSE, 2008; Padovan and Del-Col, 2010; Khan and Ahmad, 2012). Moreover, the accuracy of the transposition model varies according to the sky clearness, as the model could produce the best performance for overcast sky, but it suffered
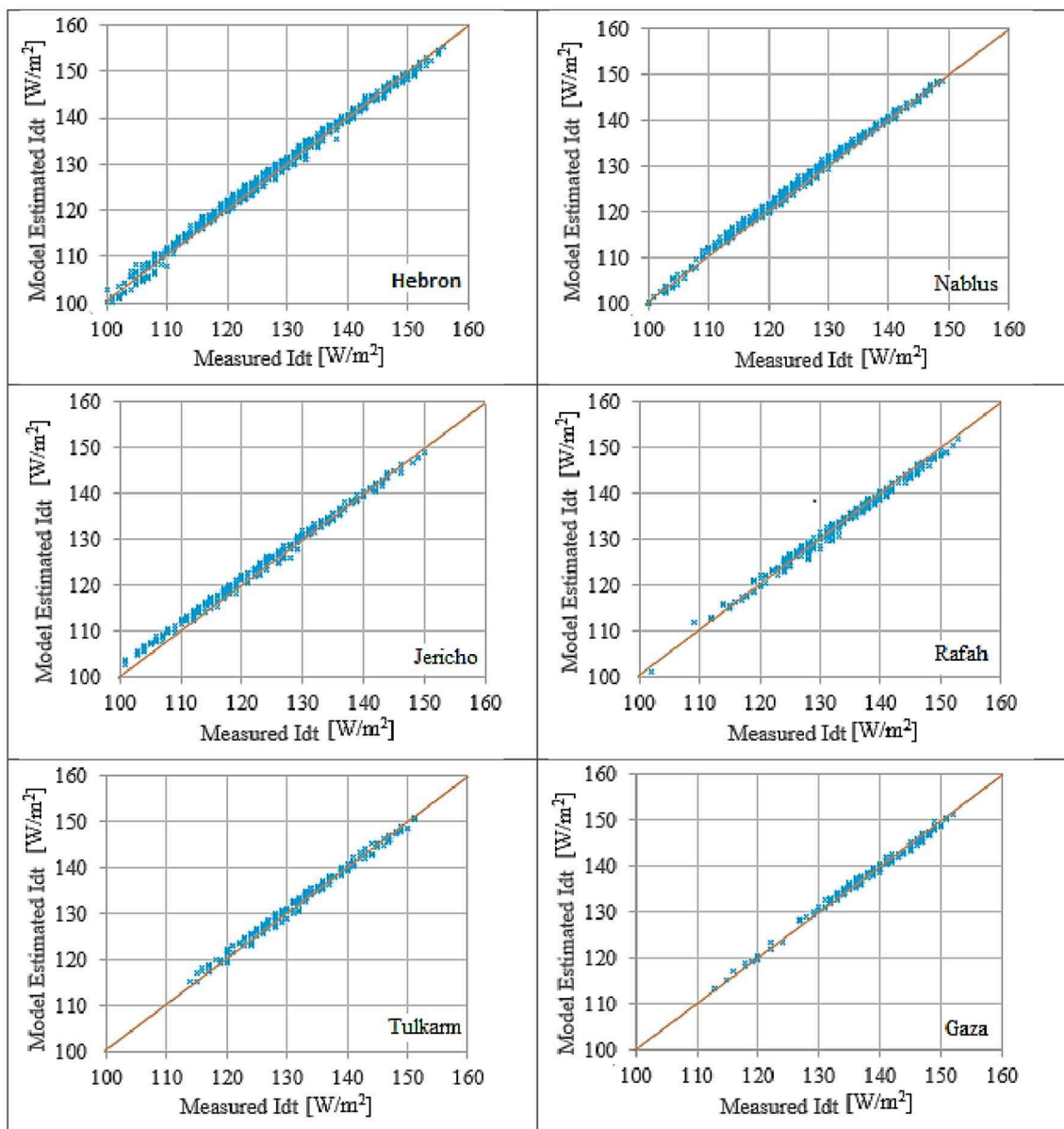
FIGURE 7 | The behavior of the modified Muneer model for clear sky condition $K_t > 0.78$ (8,700 points depicted in the graph) (blue dot), y = x relation (red line).

from deteriorated performance under clear sky conditions, **Table 5**.

2. The HDKR model showed a relatively better performance than the others for depicting the sky-diffuse inclined solar irradiance for a majority of Palestinian cities. For Nablus, however, the Skartveit-Olseth model produced a better overall performance than the other candidate models. It produced 3.4% higher than the HDKR model.

3. A majority of the investigated models suffered from inefficient performances for clear sky conditions, k_t >0.78, which represents the majority of climatological

conditions in the MENA; a robust, efficient, and reliable transposition model is therefore proposed in this article for k_t >0.78. The proposed model, as shown in **Table 6**, **Figures 5–7**, produced a better performance than the best models for different the Palestine terrains under investigation.

4. It is difficult to identify a single software that could be used for the different cities in the entire region as these software are developed according to single transposition model, **Table A2** in the appendix. A number of these are recommended for investigating the performance of solar energy projects in the Palestine

state, such as HOMER, Energypro, and PVdesignPro. Matlab Simulink is appropriate for clear sky conditions, $k_t > 0.78$.

It is worth mentioning that further investigations are required for assessing the feasibility of the studied transposition models and the proposed model for other tilt and azimuth surface angles.

DATA AVAILABILITY STATEMENT

All datasets generated for this study are included in the article/**Supplementary Material**.

AUTHOR CONTRIBUTIONS

SUPPLEMENTARY MATERIAL

The Supplementary Material for this article can be found online at: https://www.frontiersin.org/articles/10.3389/fenrg. 2019.00163/full#supplementary-material

REFERENCES

Alsadi, S., and Nassar, Y. (2016). Correction of the ASHRAE clear-sky model parameters based on solar radiation measurements in the Arabic countries. *Int. J. Renew. Energy Technol. Res.* 5, 1–16. Available online at: http://ijretr.org (accessed November 02, 2019).

Badescu (2002). 3D isotropic approximation for solar diffuse irradiance on tilted surfaces. *Renew. Energy* 26, 221–223. doi: 10.1016/S0960-1481(01)00123-9

Besharat, F., Dehghan, A., and Faghih, A. (2013). Empirical models for estimating global solar radiation: a review and case study. *Renew. Sustain. Energy Rev.* 21, 798–821. doi: 10.1016/j.rser.2012.12.043

Bilbao, J., Román, R., and De Miguel, A. (2014). "Measurements and model evaluations of direct normal irradiance in central Spain," in *Conference EuroSun 2014* (Aix-les-Bains). doi: 10.18086/eurosun.2014.08.03

Bugler, J. (1977). The determination of hourly insolation on an inclined plane using a diffuse irradiance model based on hourly measured global horizontal insolation. *Solar Energy* 19, 477–491. doi: 10.1016/0038-092X(77)90103-7

Burgess, P., Vahdati, M., Davies, D., and Philip, S. (2011). "Development of A virtual pyranometer for solar energy monitoring," in *TSBE Eng. Conference* (Whiteknights: TSBE Centre, University of Reading). Available online at: http://www.reading.ac.uk/tsbe/ (accessed November 02, 2019).

Camelia, S., and Dorin, S. (2014) Optimum tilt angle for flat plate collectors all over the World – A declination dependence formula and comparisons of three solar radiation models. *Energy Conv. Manag.* 81, 133–143. doi: 10.1016/j.enconman.2014.02.016

Chwieduk, A. (2009). Recommendation on modelling of solar energy incident on a building envelope. *Renew. Energy* 34, 736–741. doi: 10.1016/j.renene.2008.04.005

CIBSE (2008). *CIBSE Guide J.* London: Chartered Institution of Building Services Engineers.

Duffie, J., and Beckman, W. (2013). *Solar Engineering of Thermal Processes, 4th Edn.* Hoboken, NJ: John Wiley & Sons, Inc.

Escobedo, J., Souza, A., and Martins, D. (2014). An assessment of the diffuse radiation models for prediction on hourly global radiation on tilted surface. *Nativa* 2, 23–31. doi: 10.14583/2318-7670.v02n01a05

Gracia, A., and Huld, T. (2013). *Performance Comparison of Different Models for the Estimation of Global Irradiance on Inclined Surfaces, Report EUR 26075.* Brussels: European Commission; Joint Research Centre; Institute for Energy and Transport.

Gueymard, C. (1986). An anisotropic solar irradiance model for tilted surfaces and its comparison with selected engineering algorithms. *Solar Energy* 38, 367–386. doi: 10.1016/0038-092X(87)90009-0

Hafez, A., Soliman, A., El-Metwally, K., and Ismail, I. (2017). Tilt and azimuth angles in solar energy applications – a review. *Renew. Sustain. Energy Rev.* 77, 147–168. doi: 10.1016/j.rser.2017.03.131

Hay, J. (1979). *Study of Shortwave Radiation on Non-horizontal Surfaces, Downs View: Atmospheric Environment Service.* Canadian Climate Centre Report.

Hay, J. (1993). Calculating solar radiation for inclined surfaces: practical approaches. *Renew. Energy* 3, 373–380. doi: 10.1016/0960-1481(93)90104-O

Hay, J., and McKay, D. (1988). *Final Report IEA Task IX-Calculation of Solar Irradiances for Inclined Surfaces: Verification of Models Which Use Hourly and Daily Data.* Technical Report. International Energy Agency Solar Heating and Cooling Programme.

Horváth, M., and Csoknyai, T. (2015). Evaluation of solar energy calculation methods for 45o inclined, south facing surface. *Energy Proc.* 78, 465–470. doi: 10.1016/j.egypro.2015.11.700

Jimenez, J., and Castro, Y. (1986). *National Assembly of Geophysics and Geodesy*, Vol. II, 805.

Kasten, F. (1966). A new table and approximate formula for relative optical air mass. *Arch. Meteorol. Geophys. Bioklimatal. Series B* 14, 206–223. doi: 10.1007/BF02248840

Khan, M., and Ahmad, M. (2012). Estimation of global solar radiation using clear sky radiation in Yemen. *J Eng. Sci. Technol. Rev.* 5, 12–19. doi: 10.25103/jestr.052.03

Khatib, T., Mohamed, A., Mahmoud, M., and Sopian, K. (2015). Optimization of the tilt angle of solar panels for Malaysia. *Energy Sources* 37, 606–613. doi: 10.1080/15567036.2011.588680

Klucher, T. (1979). Evaluation of models to predict insolation on tilted surfaces. *Solar Energy* 23, 111–114. doi: 10.1016/0038-092X(79)90110-5

Koronakis, P. (1986). On the choice of the angle of tilt for south facing solar collectors in the Athens basin area. *Solar Energy* 36, 217–225. doi: 10.1016/0038-092X(86)90137-4

Lave, M., Hayes, M., Pohl, A., and Hansen, C. (2015). Evaluation of global horizontal irradiance to plane-of-array irradiance models at locations across the united states. *IEEE J.* Photovolt. 5, 597–606. doi: 10.1109/JPHOTOV.2015.2392938

Liu, B., and Jordan, R. (1963). The long-term average performance of flat-plate solar energy collectors. *Solar Energy* 7, 53–74. doi: 10.1016/0038-092X(63)90006-9

Ma, C. (1983). Statistical comparison of models for estimating solar radiation on inclined surfaces. *Solar Energy* 31, 313–317. doi: 10.1016/0038-092X(83)90019-1

Michael, S., Okundamiya, J., Emagbetere, O., and Emmanuel, A. (2016). Evaluation of various global solar radiation models for Nigeria. *Int. J. Green Energy* 13, 505–512. doi: 10.1080/15435075.2014.968921

Moretón, R., Lorenzo, E., Pinto, A., Muñoa, J., and Narvarte, L. (2017). From broadband horizontal to effective inplane irradiation: a review of modelling and derived uncertainty for PV yield prediction. *Renew. Sustain. Energy Rev.* 78, 886–903. doi: 10.1016/j.rser.2017.05.020

Muneer, T. (1990). Solar radiation models for Europe. *Build. Serv. Eng. Res. Technol.* 11, 153–163. doi: 10.1177/014362449001100405

Muneer, T. (1997) *Solar Radiation and Daylight Models for the Energy Efficient Design of Buildings.* Oxford; Boston, MA: Architectural Press. 197–200.

Muneer, T., Gueymard, C., and Kambezidis, H. (2004). "Hourly slope irradiation and illuminance," in *Solar Radiation and Daylight Models,* ed G. M. Alam (Oxford: Butterworth-Heinemann), 143–221. doi: 10.1016/B978-075065974-1/50012-7

Nassar, Y. (2006). *Solar Energy Engineering Active Applications.* Libya: Sebha University.

Noorian, A., Moradi, I., and Kamali, G. (2008). Evaluation of 12 models to estimate hourly diffuse irradiation on inclined surfaces. *Renew. Energy* 33, 1406–1412. doi: 10.1016/j.renene.2007.06.027

Olmo, F., Vida, J., Foyo, I., Castro-Diez, Y., and Alados-Arboledas, L. (1999). Prediction of global irradiance on inclined surfaces from horizontal global irradiance. *Energy* 24, 689–704. doi: 10.1016/S0360-5442(99)00025-0

Padovan, A., and Del-Col, D. (2010). Measurement and modelling of solar irradiance components on horizontal and tilted planes. *Solar Energy* 84, 2068–2084. doi: 10.1016/j.solener.2010.09.009

Pandey, C., and Katiyar, A. (2014). Hourly solar radiation on inclined surfaces. *Sust. Energy Technol. Assess.* 6, 86–92. doi: 10.1016/j.seta.2014.01.007

Perez, R., and Arbogast, C. (1985). "Climatology of an anisotropic diffuse sky radiation model for slopes," in *Proceedings ISES Word Congress* (Montreal, QC). doi: 10.1016/B978-0-08-033177-5.50470-1

Perez, R., Arbogast, C., Seals, P., and Scott, J. (1986). An anisotropic hourly diffuse radiation model for sloping surfaces: description, performance validation, site dependency evaluation. *Solar Energy* 36, 487–497. doi: 10.1016/0038-092X(86)90013-7

Perez, R., and Scott, J. (1983). "A two-parameter description of the sky hemisphere," in *Proceedings of ISES/AMS Fifth Conference on Atmospheric Radiation*, Baltimore, MD (Boston: American Meteorological Society), 322–325.

Perez, R., Seals, R., Ineichen, P., and Menicucci, D. (1987b). A new simplified version of the Perez diffuse irradiance model for tilted surfaces. *Solar Energy* 39, 22l–231. doi: 10.1016/S0038-092X(87)80031-2

Perez, R., Seals, R., Ineichen, P., Stewart, R., and Michalsky, J. (1990a). Modelling daylight availability and irradiance components from direct and global irradiance. *Solar Energy* 44, 271–289. doi: 10.1016/0038-092X(90)90055-H

Perez, R., Seals, R., and Stewart, R. (1987a). "Modelling irradiance on tilted planes: a simpler version of the Perez model: US-wide climatic/environmental evaluation," in *Advances in Solar Energy Technology ISES World Congress, Ham burg.* (New York, NY: Pergamon Press), 3784–3788. doi: 10.1016/B978-0-08-034315-0.50698-4

Perez, R., Seals, R., Zelenka, A., and Ineichen, P. (1990b). Climatic evaluation of models that predict hourly direct irradiance from hourly global irradiance: prospects for performance improvements. *Solar Energy* 44, 99–108. doi: 10.1016/0038-092X(90)90071-J

Perez, R., and Stewart, R. (1983). "An anisotropic model for diffuse radiation incident on slopes of different orientations and possible applications to CPCs," in *Proceeding of ASES Minneapolis.* (Minneapolis, MN), 883–888.

Perez, R., Stewart, R., and Guertin, T. (1988). *Sandia National Laboratories Contractor Report SAND88-7030 Oct.* (1988). The Development and veriFication of the Perez Diffuse Radiation Model. Albuquerque, NM. doi: 10.2172/7024029

Pérez-Burgos, A., Díez-Mediavilla, M., Alonso-Tristán, C., and Dieste-Velasco, M. (2018). Retrieval of monthly average hourly values of direct and diffuse solar irradiance from measurements of global radiation in Spain. *J. Renew. Sustain. Energy* 10:023707. doi: 10.1063/1.5016926

Psiloglou, B., and Kambezidis, H. (2009). Estimation of the ground albedo for the Athens area, Greece. *J. Atmos. Solar Terrestr. Phys.* 71, 943–954. doi: 10.1016/j.jastp.2009.03.017

Raptis, P., Kazadzis, S., Psiloglou, B., Kouremeti, N., Kosmopoulos, P., and Kazantzidis, A. (2017). Measurements and model simulations of solar radiation

at tilted planes, towards the maximization of energy capture. *Energy* 130, 570–580. doi: 10.1016/j.energy.2017.04.122

Reindl, D., Beckman, W., and Duffie, J. (1990a). Diffuse fraction correlations. *Solar Energy* 45, 1–7. doi: 10.1016/0038-092X(90)90060-P

Reindl, D., Beckman, W., and Duffie, J. (1990b). Evaluation of hourly tilted surface radiation models. *Solar Energy* 45, 9–17. doi: 10.1016/0038-092X(90)90061-G

Skartveit, A., and Olseth, J. (1986). Modelling slope irradiance at high latitudes. *Solar Energy* 36, 333–344. doi: 10.1016/0038-092X(86)90151-9

Steven, M., and Unsworth, M. (1979). The diffuse solar irradiance of slopes under cloudless skies. *Quart. J. Roy. Meteorol. Soc.* 105, 593–602. doi: 10.1002/qj.49710544507

Steven, M., and Unsworth, M. (1980). The angular distribution and interception of diffuse solar radiation below overcast skies. *Quart. J. Roy. Meteorol. Soc.* 106, 57–61. doi: 10.1002/qj.49710644705

Temps, R., and Coulson, K. (1977). Solar radiation incident upon slopes of different orientation. *Solar Energy* 19, 179–184. doi: 10.1016/0038-092X(77)90056-1

Tian, Y., Davies-Colley, R., Gong, P., and Thorrold, B. (2001). Estimating solar radiation on slopes of arbitrary aspect. *Agric. Forest Meteorol.* 109, 67–74. doi: 10.1016/S0168-1923(01)00245-3

Togrul, I. (1989). Comparison of statistical performance of seven sunshine based models for Elazig, Turkey. *Chim. Acta Turcicam.* 1, 26–37.

Tuomiranta, A., and Ghedira, H. (2015). "Evaluation of decomposition and transposition models for irradiance data conversion under a hot desert climate," in *3rd International Conference Energy and Meteorology* (Boulder, CO).

Ulgen, K., and Hepbasli, A. (2004). Solar radiation models. Part 1: a review. *Energy Sourc.* 26, 507–520. doi: 10.1080/009083104904 29696

Vasar, C., Prostean, O., and Prostean, G. (2016). Evaluating solar radiation on tilted surfaces – a study case in Timis (Romania). *IOP Conf. Ser. Mater. Sci. Eng.* 106:012026. doi: 10.1088/1757-899X/106/1/012026

Willmot, C. (1982). On the climatic optimization of the tilt and azimuth of flat-plate solar collectors. *Solar Energy* 28, 205–216. doi: 10.1016/0038-092X(82)90159-1

Yadav, A., Chandel, S. S. (2013). Tilt angle optimization to maximize incident solar radiation: a review. *Renew. Sust. Energy Rev.* 23, 503–513. doi: 10.1016/j.rser.2013.02.027

Zhang, J., Zhao, L., Deng, S., Xu, W., and Zhang, Y. (2017). A critical review of the models used to estimate solar radiation. *Renew. Sustain. Energy Rev.* 70, 314–329. doi: 10.1016/j.rser.2016.11.124

NOMENCLATURE

F1	Circumsolar brightness coefficient
F2	Horizon brightness coefficient
Fij	Perez simplified model coefficient
Ih	Global solar irradiance on a horizontal plane, W/m2
Ibh	Direct beam irradiance on a horizontal plane, W/m2
Idh	Sky-diffuse irradiance on a horizontal plane, W/m2
IDN	Direct normal solar irradiance, W/m2
It	Global solar irradiance on an inclined plane, W/m2
Ibt	Direct beam irradiance on an inclined plane, W/m2
Idt	Sky -diffuse irradiance on an inclined plane, W/m2
Irt	Ground-reflected irradiance on an inclined plane, W/m2
Isc	Solar constant (1367 W/m2)
Iext	Extraterrestrial solar irradiance, W/m2
Ii,c	Calculated solar irradiance for time i, W/m2
Ii,m	Measured solar irradiance for time i, W/m2
Kt	Hourly clearness index
M	Optical air mass
N	Number of data
Rb	Direct beam transposition factor
Rd	Sky-diffuse transposition factor
Rr	Ground-reflected transposition factor
ρg	Ground reflectivity or albedo
Δ	Brightness index
ε	Sky clearness index
β	Surface inclination
ψ	Surface azimuth angle
Θz	Solar zenith angle
Θi	Solar incident angle
γ	Solar altitude angle